# Chapter 3

# Experimental Setups

## 3.1 Synchrotron Radiation Experiments

The synchrotron radiation sources have been developed significantly over the last decade. Starting from first generation parasitic use of nuclear and high energy physics machines, to second generation dedicated storage rings, to third generation facilities with insertion devices. Now we are witnessing even larger jumps in brightness (as shown in Fig.3.1) due to the implementation of multiparticle coherence in fourth generation accelerators. Moreover, the spectral range accessible via synchrotron radiation is also expanded: with the first experiments using the visible spectral range up to x-rays down to about half an Ångestrom, this range is expanded to both sides. Now synchrotron generated infrared radiation yields higher intensity than all other sources, and the hard x-ray range spans up to several hundred keV. In this part, I would like to give a short overview about the synchrotron light source, beam lines, and the experiment setups which have been used in this study.

### 3.1.1 Synchrotron Light

In light sources, we make use of the fact that when charged particles are accelerated, they emit light (radiate). If electrons are accelerated back and forth in an antenna at kilohertz or Megahertz frequencies they radiate in the radio or TV range of the electromagnetic spectrum. If electrons are constrained to move in a curved path (circles, spirals, and undulations are examples) they are accelerated toward the inside of the curve and will also radiate what we call synchrotron light (or synchrotron radiation). Synchrotron light is unique in its intensity and brilliance and it can be generated across a wide range of the electromagnetic spectrum: from infrared to x-rays, as shown in Fig.3.2.
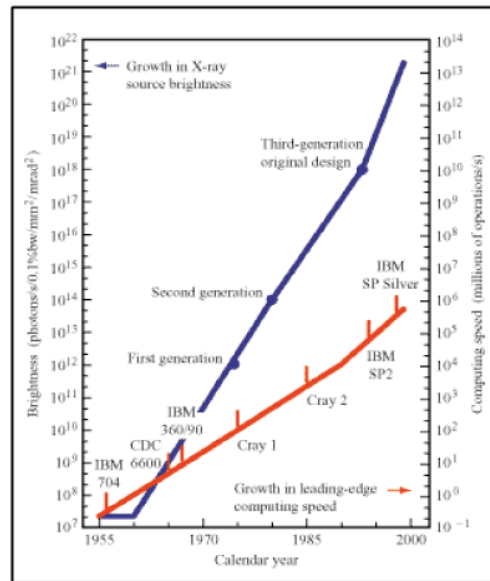
Figure 3.1: Increase since 1955 in X-ray source brightness (blue) and growth in leading-edge computing speed (red) (taken from SRN of December 2006).
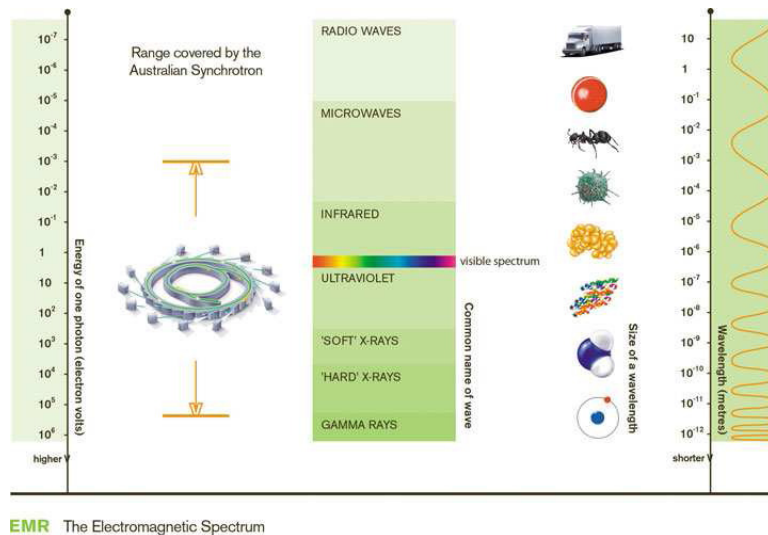


Figure 3.2: Range of light cover by the BESSYII synchrotron (Taken from BESSY homepage).

Synchrotron radiation is not only man made, it exists in nature. Magnetic field have been detected in solar sunspots by Hale (1908) by observing the Zeeman splitting of optical spectral lines. Davis and Greenstein (1951) developed an interpretation that suggested that the optical polarization was due to dust grains aligned by magnetic fields of the Milky Way. Thus one of the requirements for synchrotron radiation, the presence of cosmic magnetic fields, had been established. The mysterious radio-stars were identified by Bolton et al. (1949) with such diverse cosmic objects as a historical supernova remnant (Crab Nebula, as shown in Fig.3.3), a nearby galaxy (Centaurus A), and a distant galaxy with a jet (Virgo A). The Crab Nebula turned out to be the Rosetta-stone of astrophysics, leading to the establishment of the synchrotron theory as a basis of modern astrophysics.



Figure 3.3: The Crab Nebula. Visible synchrotron emission from the Crab Nebula is shown as the diffuse blue region in the interior of the nebula. The network of filaments shown as red and green are composed of ejecta from the supernova that have been swept up and photoionized by the expanding synchrotron nebular. (ESA, NASA, J. Hester and A. Loll, Arizona State University.)

Producing synchrotron radiation at BESSY II requires coordination of several systems. A primary accelerating system to accelerate an electron beam, a storage ring to store the electrons for several hours together with so-called insertion devices (IDs) to produce the radiation; beam line systems with monochromator to tune and direct the radiation to an experimental end-station where the research work and computer aided evaluation of the data is carried out. The accelerator

system at BESSY is very typical for synchrotron radiation facilities. It is almost just as in a TV tube electrons are emitted by a hot cathode (e.g. a hot filament) in high vacuum. They are accelerated to an energy of 100 keV by an anode voltage of 100 000 Volts. The second accelerating stage is a microtron, the center part of which is a linear accelerator with a strong high frequency electrical field. The electrons pass through this field ten times as they are redirected on larger growing trajectories by a strong constant magnetic field until they achieve an energy of 50 million eV (50 MeV). From there the electrons are passed into the vacuum chamber of the synchrotron accelerator. A closed system of tubes with a diameter of 4 x 8 cm and 96 meters in circumference. The electrons are focused on the correct trajectory or orbit by strong magnets and are accelerated by the alternating field of a cavity resonator to the final energy of 1.7 Giga electron-volts (1.7 GeV or 1700 MeV). To keep the electrons on the correct trajectory as they approach to the speed of light the strength of the magnetic fields is increased as the kinetic energy increases. This cyclic acceleration occurs at a frequency of 10 Hertz, i.e. ten times per second some 10 billion electrons are accelerated to the final energy. Then the electrons are injected via a transfer channel into the storage ring. More details about the ring operation, can be found at BESSY homepage.

### 3.1.2  Beam Line

The light from the synchrotron radiation leaves the storage ring on a tangential path through the radiation outlets (front ends) into the beam lines at BESSY. The beam lines can be up to 40 meters long. In the beam lines the radiation is directed by optical elements through monochromator to the experimental end stations. Monochromator work like filters to select a certain band pass of wavelengths out of the emitted spectrum. The light beam can be focused with curved mirrors. Since many beam lines and monochromator can be set up at a storage ring many experiments can be carried out simultaneously. For each of the investigations the wavelength of the light and the experimental requirements can be individually set. At BESSY up to 50 such experimental stations for independent external research can be set up and operated simultaneously. A schematic presentation of insertion device beamline is presented in Fig.3.4.
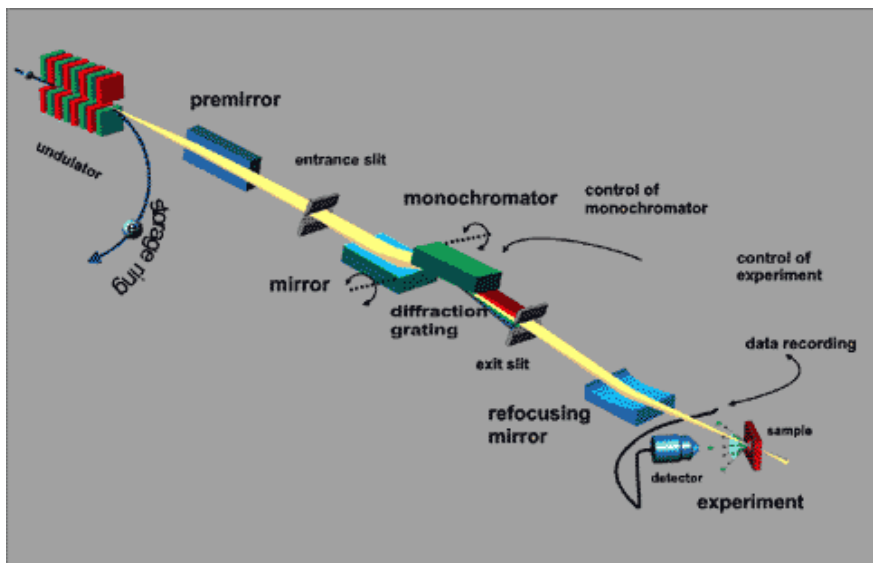
Figure 3.4: Typical path of the light beam from the source to the sample at BESSY. (Taken from BESSY homepage)

## 3.2   XAS of Liquid Samples (LIQUIDROM)

The LIQUIDROM setup consists of two main parts, differential pumping stage, and main chamber, as shown in Fig.3.5. Light from the synchrotron enters the chamber through the differential pumping which separate the UHV on the beamline side, from the HV of the experimental chamber. X-rays enter the chamber through a thin membrane, which separates the atmospheric pressure in the chamber from the HV pressure in the second half of the differential pumping. Many kinds of membranes can be used, like carbon, $Si_3N_4$, as well as Al membranes. Choosing the membrane depends on the desired edge that needs to be investigated in the solution. The liquid sample is introduced into the chamber as a highly pressurized jet, which is circulated by peristaltic pump. X-rays impinge the liquid jet inside the main chamber and total fluorescence yield (TFY) is measured with a GaAs photodiode. Recently, total electron yield (TEY) could also be measured by applying a highly positive potential to a copper plate placed within 5 mm from the liquid jet.
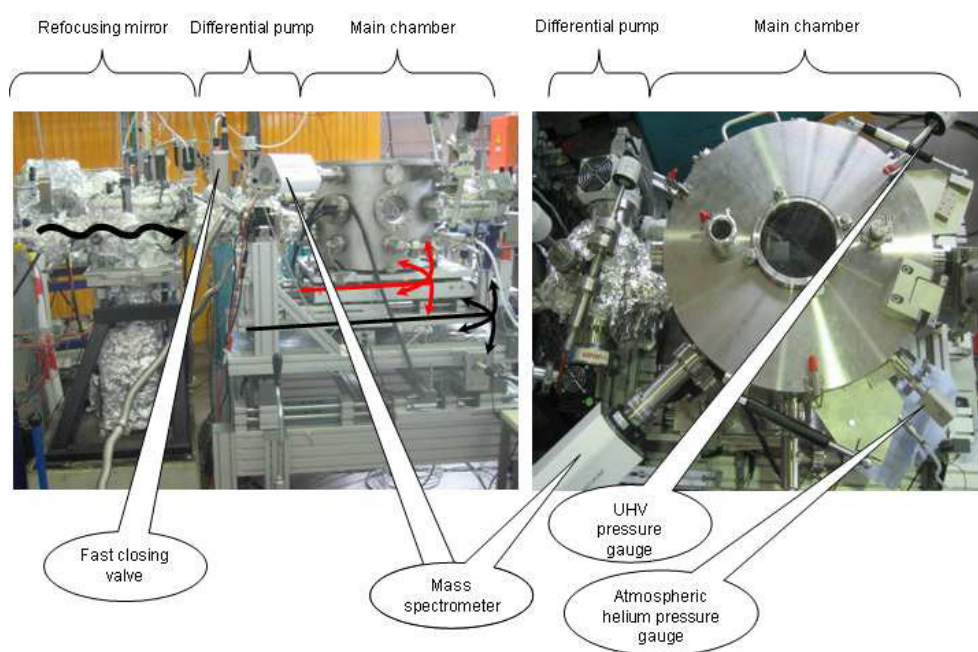


Figure 3.5: Side view of the LIQUIDROM setup (right), and top view (left).

For particularly volatile solvent (e.g. alcohol) the solution is flowed through

a closed cell (see Fig.3.6). A membrane separates the liquid from the chamber which can now be pumped to HV. In this case the membrane separated the differential pumping state from the chamber can be omitted. In case of the membrane being damaged or cracked, the pressure in the main chamber will increase, and so does the pressure in the first differential pumping stage. A pressure sensor connected to the first part of the differential pumping will immediately shut the fast closing valve upon a pressure rise higher than $10^{-4}$ mbar
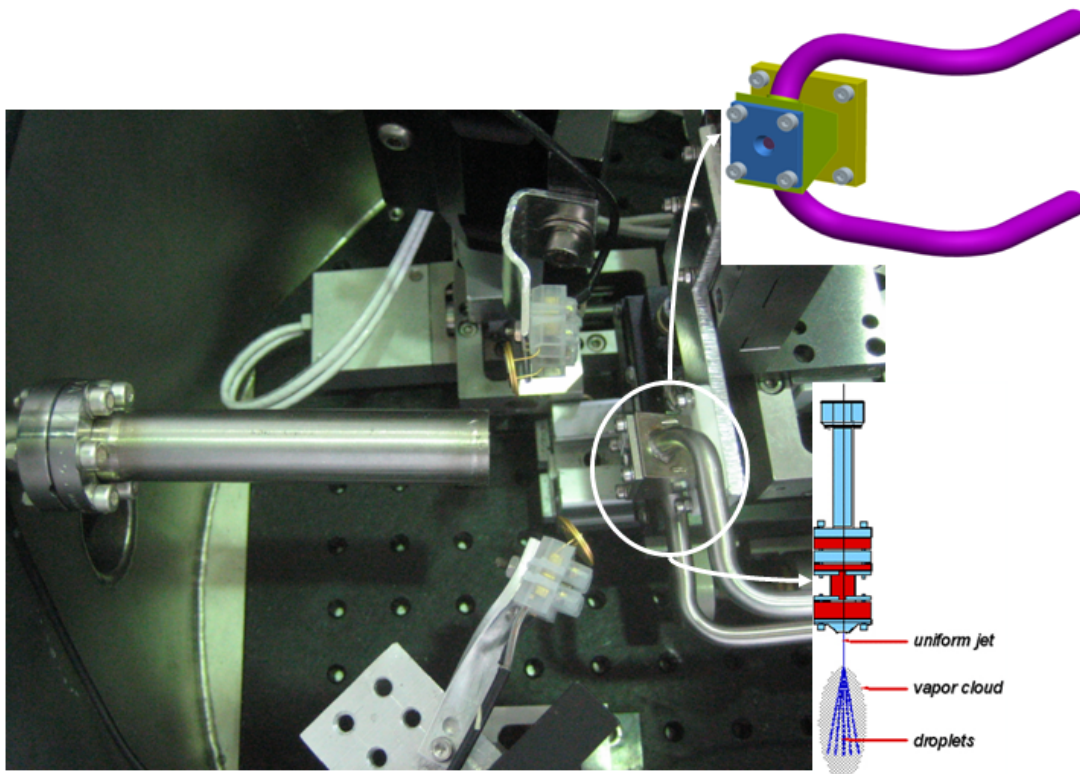


Figure 3.6: Details picture for the LIQUIDROM chamber. The flow cell of volatile solution is presented in the right corner top, and for the non-volatile ones in the right corner bottom.

## 3.3   RIXS of Liquid Samples

RIXS spectra were recorded using a high-resolution grazing-incidence grating spectrometer at the advanced light source [61]. It is based on Rowland geometry, which achieves both wavelength dispersion and focusing in a single step. It consists of slit, gratings and a detector. Three spherical gratings are optimized to cover an operation range from 50 to 1000 eV, as shown in Fig.3.7. X-rays are detected by a two-dimensional detector which can be positioned and oriented tangentially to the Rowland circle. The detector is placed inside a housing, which is mounted in such a way that it can be moved along two perpendicular spatial axes. The detector can also be rotated around an axis parallel to the detector surface in order to stay tangential to the Rowland circle for all detector positions.
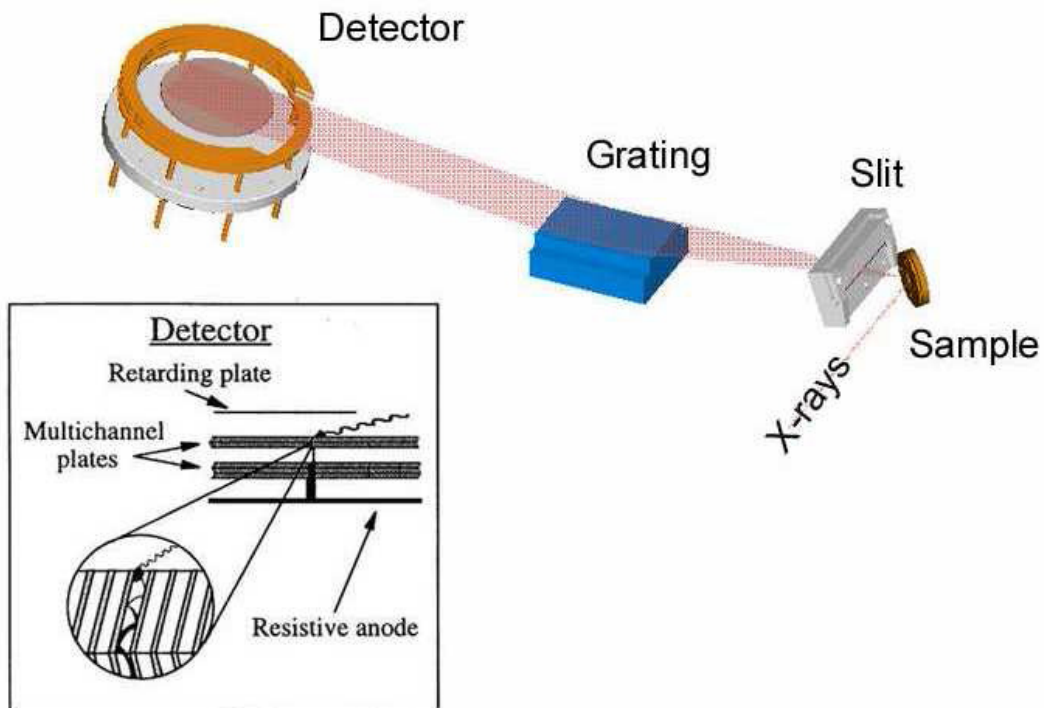


Figure 3.7: Schematic illustration of the soft x-ray spectrometer presented with one grating. (Taken from Jinghua Guo, private communication.)

The liquid is kept in a small vacuum tight container as shown in Fig.3.8, where the x-rays penetrate through a thin membrane window. This very thin membrane

of 2.5 x 2.5 mm$^2$ can withstand a pressure difference of one atmosphere. The cell consists of a two piece metal or plastic container, which is sealed using a standard o-ring placed between the back of the cell and the window.
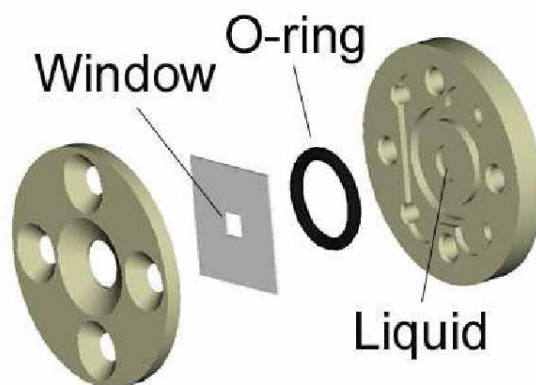


Figure 3.8: Schematic illustration of the cell used for liquid measurements. The liquid is separated from the vacuum by a 150 nm thick silicon nitride window. (Taken from Jinghua Guo, private communication.)

## 3.4   XPS of Liquid Samples

The synchrotron light interacts with a laminar liquid jet at normal incidence with respect to the liquid-jet flow direction, and electron detection is normal to both the jet direction and the light polarization vector as shown in Fig.3.9. Photoelectrons pass through a 100-$\mu$m orifice that separates the jet main chamber ($10^{-5}$ mbar) from the electron detection chamber ($10^{-9}$ mbar). The latter houses a hemispherical electron energy analyzer, equipped with a single electron multiplier detector (which was recently replaced by a multichannel detector). This chamber is pumped by two turbomolecular pumps. The working pressure in the jet chamber, $10^{-5}$ mbar, is maintained using a set of liquid-nitrogen cold traps, in addition to a 1500 L/s turbomolecular pump. A differential pumping stage connects the liquid-jet main chamber and the end chamber of the beamline ($10^{-9}$ mbar), housing the refocusing mirrors, with the same principle as it discussed in section 3.2. Helmholtz coils were used to compensate for the Earth's magnetic field.
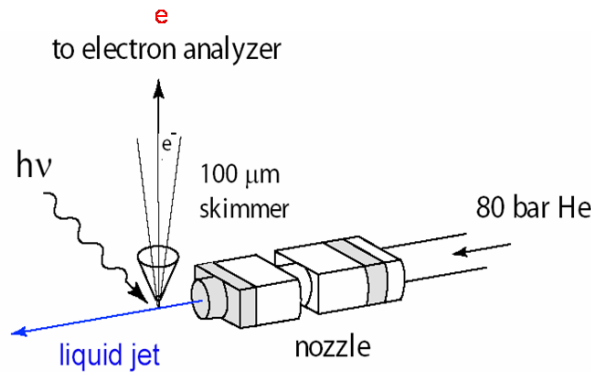


Figure 3.9: Experimental setup of the liquid microjet photoemission experiment. The polarization vector of the synchrotron light E is perpendicular to the direction of electron detection and parallel to the direction of jet propagation. Photoelectrons pass through the skimmer, acting as differential pump, at the entrance of a hemispherical electron energy analyzer. The pressure in the interaction chamber is $\approx 10^{-5}$ mbar, and the jet velocity is 120 $ms^{-1}$. (The picture taken from REF. [15])